Ultrasonics Sonochemistry 94 (2023) 106345

Contents lists available at ScienceDirect

Ultrasonics Sonochemistry

journal homepage: www.elsevier.com/locate/ultson

In situ studies on free-standing synthesis of nanocatalysts via acoustic levitation coupled with pulsed laser irradiation

Juhyeon Park [a,1], Ahreum Min [b,1], Jayaraman Theerthagiri [a,1], Muthupandian Ashokkumar [c,*], Myong Yong Choi [a,b,*]

[a] Department of Chemistry (BK21 FOUR), Research Institute of Natural Sciences, Gyeongsang National University, Jinju 52828, Republic of Korea
[b] Core-Facility Center for Photochemistry & Nanomaterials, Gyeongsang National University, Jinju 52828, Republic of Korea
[c] School of Chemistry, University of Melbourne, Parkville Campus, Melbourne, VIC 3010, Australia

ARTICLE INFO

Keywords:
Acoustic levitation
Gold and silver nanoparticles
In situ spectroscopy
4-nitrophenol reduction
Pulsed laser irradiation

ABSTRACT

Acoustic levitation is a distinctive and versatile tool for levitating and processing free-standing single droplets and particles. Liquid droplets suspended in an acoustic standing wave provide container-free environments for understanding chemical reactions by avoiding boundary effects and solid surfaces. We attempted to use this strategy for the production of well-dispersed uniform catalytic nanomaterials in an ultraclean confined area without the addition of external reducing agents or surfactants. In this study, we report on the synthesis of gold and silver nanoparticles (NPs) via acoustic levitation coupled with pulsed laser irradiation (PLI). *In situ* UV–Visible and Raman spectroscopic techniques were performed to monitor the formation and growth of gold and silver NPs. The PLI was used for the photoreduction of targeted metal ions present in the levitated droplets to generate metal NPs. Additionally, the cavitation effect and bubble movement accelerate the nucleation and decrease the size of NPs. The synthesized Au NPs with ~ 5 nm size showed excellent catalytic behavior towards the conversion of 4-nitrophenol to 4-aminophenol. This study may open a new door for synthesizing various functional nanocatalysts and for achieving new chemical reactions in suspended droplets.

1. Introduction

Acoustic levitation is an exciting technique for container-free sample handling by levitating samples of interest in a field of sound waves generated by an emitter and reflector. For this container-less process, liquid and solid samples can be placed in an ideal free-standing environment utilizing an ultrasonic standing wave [1,2]. The droplet volume in the levitated system can be in the microliter range, which is larger when compared with other levitated systems, such as electrostatic or optical levitation. The levitated droplet volume is dependent on the ultrasonic frequency; lower frequencies permit a large levitated droplet volume. Solvent evaporation during levitation slowly decreases the droplet volume and thus increases the resulting solute concentration [3]. Acoustic levitation is suitable for a wide range of substances and is not restricted to any particular sample or shape. The major benefits of such a levitation process lie in eliminating the complicated impacts caused by the contacting wall or surface on the sample [4]. The contact between the chemical agent and container in the normal wet chemistry route triggers heterogeneous nucleation. Moreover, interfaces of solid–liquid boundaries can affect the uniformity of particle growth during solvent evaporation [5].

Furthermore, the contamination of samples can be eradicated by the absence of container walls or contacting surfaces. Additionally, the resulting samples can be applied for analytical techniques with enhanced sensitivity for combined spectroscopic characterization tools with acoustic levitators, such as UV–Vis spectroscopy, FT-IR spectroscopy, and Raman spectroscopy, and X-ray diffraction, employed to investigate the physical and chemical amendments of the levitated droplets [2]. This versatility creates acoustic levitation, a remarkable emerging tool in materials science, astrochemistry, analytical chemistry, and pharmaceuticals. Acoustic levitation can also initiate a chemical reactions by mixing two droplets containing different reagents [6]. Moreover, acoustic levitation is increasingly attracting attention in the space research community for low-gravity simulation testing. The

* Corresponding authors at: Department of Chemistry (BK21 FOUR), Research Institute of Natural Sciences, Gyeongsang National University, Jinju 52828, Republic of Korea (M.Y. Choi).
E-mail addresses: masho@unimelb.edu.au (M. Ashokkumar), mychoi@gnu.ac.kr (M.Y. Choi).
[1] These authors contributed equally to this work.

https://doi.org/10.1016/j.ultsonch.2023.106345
Received 17 November 2022; Received in revised form 21 February 2023; Accepted 23 February 2023
Available online 26 February 2023

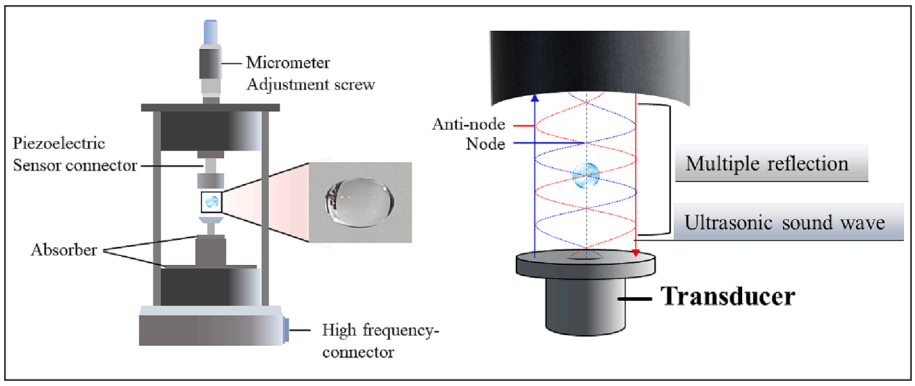

Fig. 1. Typical free-standing acoustic droplet in acoustic levitator system (left) and the principle of acoustic levitator (right).

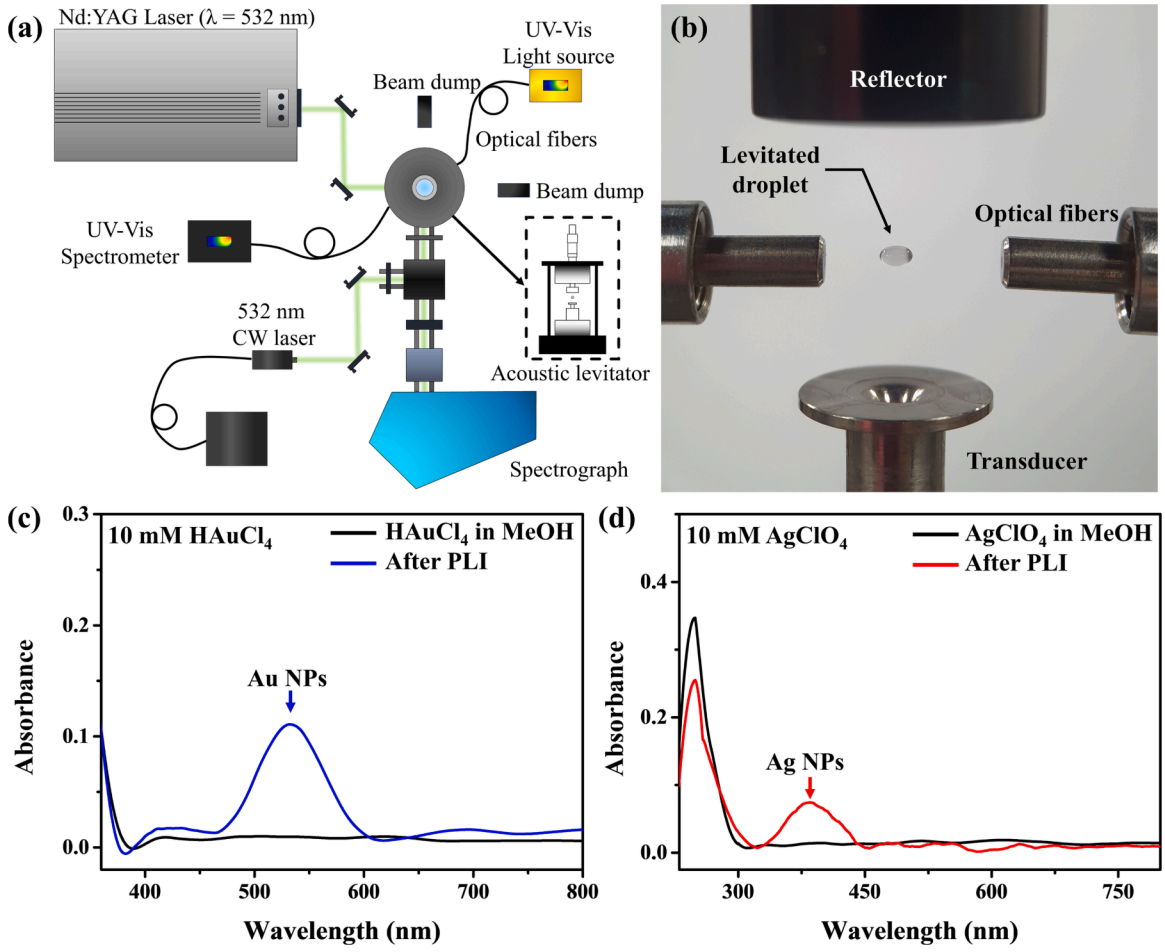

Fig. 2. (a) Detailed experimental setup of acoustic levitator system coupled with PLI and *in situ* spectroscoic techniques, (b) free-standing-leviated droplet between the ultrasonic levitator emitter and reflector in acoustic levitator, and (c and d) UV–Vis spectra of Au and Ag NPs synthesized using the acoustic levitator system coupled with the PLI process.

capability to levitate droplets or particles with a certain gas medium delivers ideal free-standing environments for simulating planetary dust particles and micrometeoroids present in the atmospheres of exoplanets and planets [4,7].

Au and Ag nanoparticles (NPs) have attracted substantial research interest because of their characteristic size and shape-dependent catalytic, optical, and antimicrobial properties [8–13]. Mostly, Au and Ag NPs are mainly synthesized by employing chemical reduction using strong reducing agents, such as $NaBH_4$ and sodium citrate. Another method involves the ultrasound waves or microwave heating of the corresponding metal salts solution in the presence of surfactants or capping agents to control the size, stability, and shape of the NPs [8,14–16]. The pulsed laser irradiation (PLI) technique has recently been employed to reduce Au and Ag salts into corresponding NPs [13,17,18]. The PLI technique possesses several advantages over chemical and other physical routes, such as rapid synthetic routes, no byproducts; moreover, it does not require toxic reducing agents or capping agents [10,19–24]. In the case of water as a solvent, hydrogen radicals act as strong reducing agents during PLI of metal salts dissolved in suitable solvents, which disintegrate and form hydrogen and hydroxyl

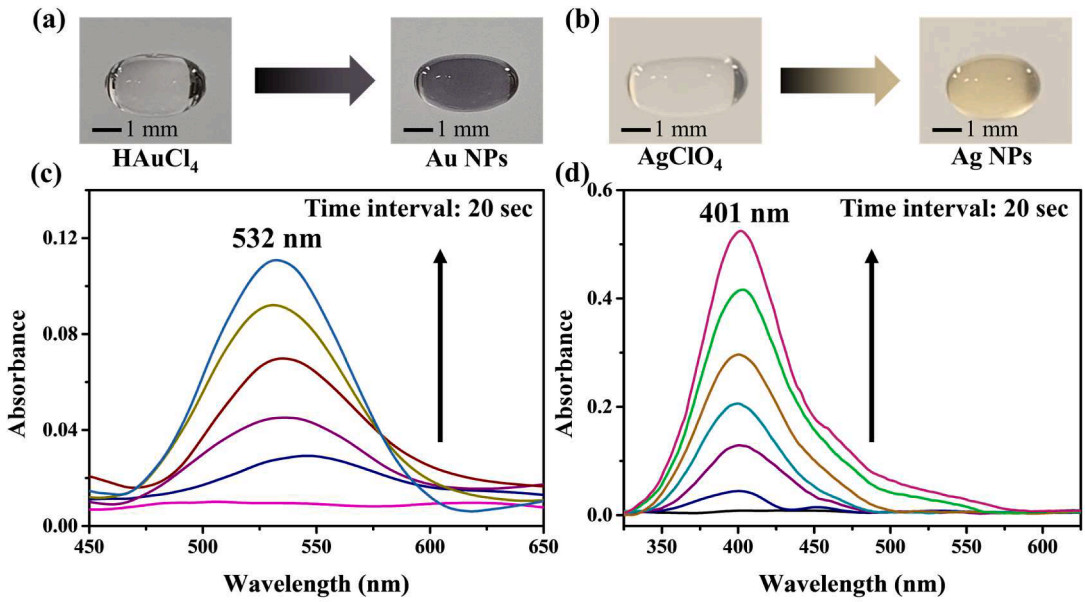

Fig. 3. (a and b) Real image of the levitated droplet captured during reduction of metal salts into Au and Ag NPs by a high-resolution camera and (c and d) kinetics of SPR peak intensities of Au^{3+} and Ag^{+} salt solution reduction with respect to PLI time.

radicals [17,19].

Herein, we report the synthesis of Au and Ag NPs via acoustic levitation coupled with PLI. Moreover, *in situ* UV–Vis and Raman spectroscopic techniques were simultaneously performed to investigate the formation and growth of NPs, as well as effects on their aggregation. A high-resolution camera monitored the oscillation and mobility of the levitated samples. The Au NPs synthesized via acoustic levitation under an optimal condition showed the characteristics of small particle size, spherical surface, and excellent catalytic behavior toward the reduction of 4-nitrophenol (4-NP) into 4-aminophenol (4-AP). We also proposed the catalytic reduction of the 4-NP mechanism over the synthesized Au NPs and compared their performance with reported catalysts synthesized by other techniques. Nitroaromatic molecules (4-NP) were taken as model organic pollutants for testing the catalytic efficiency since 4-NP is widely utilized in the field of pharmaceuticals, dyes, explosives, pesticides, and industrial chemicals, and these wastages are commonly discharged into the aquatic environment. However, several techniques, such as photocatalysis, adsorption, and electrochemical methods, are employed to remove nitroaromatic pollutants, which are restricted for large-scale applications due to high cost, slow reaction kinetics, and low degradation efficiency [25–28]. In this regard, reducing the nitroaromatic compounds over the catalyst is a feasible choice to control the aquatic environment.

2. Experimental section

2.1. Materials

Gold (III) chloride trihydrate ($HAuCl_4{\cdot}3H_2O$, ≥ 99.9%), silver perchlorate ($AgClO_4$, 99%), sodium borohydride ($NaBH_4$, ≥ 98), and 4-nitrophenol (≥99) were acquired from Sigma-Aldrich, USA. Methanol (HPLC grade solvent) was obtained from Daejong Chemicals, Korea. All reagents and materials were employed as purchased.

2.2. Synthesis of Au and Ag nanocatalysts

The Au and Ag NPs were synthesized using an ultrasonic levitator coupled with the PLI process. In a typical synthesis of Au NPs, 10 mM Au salt methanolic solution was prepared by dissolving $HAuCl_4{\cdot}3H_2O$ in 3.0 mL methanol. Then, 10 μL of Au salt methanolic solution was suspended in an acoustic standing wave chamber within an ultrasonic levitator emitter and reflector (tec5 AG acoustic levitator, Germany; 58 kHz, 166 W) using a micropipette. Subsequently, the levitated droplet was irradiated for 2 min by the unfocused pulsed laser beam with optimal conditions of Nd:YAG light source with a 532-nm wavelength, 80-mJ power, and a 7-ns pulse width at 10 Hz repetition rate (Surelite II-10). Finally, the ensuing Au colloidal sample was removed from the acoustic levitation by a micropipette and collected in a 2-mL vial. Successively, Au NPs were obtained by centrifugation, washed thoroughly with methanol, and dried at an ambient temperature. The above process was repeated several times to collect a high yield of Au NPs.

Similarly, Ag NPs were obtained by the same procedure mentioned above for Au NPs by replacing the Au metal salt with the Ag metal salt. Additionally, control experiments were also performed without PLI process, confirming that there was no reduction of metal salts into metal NPs, as shown in the UV–Vis spectra (**Figure S1** of Supporting Information).

2.3. Characterization techniques

In situ UV–Vis spectroscopy (StellarNet Black comet, USA)-coupled acoustic levitator was utilized to monitor and analyze the reduction of the metal salt into metal NPs, and also the catalytic conversion of 4-NP to 4-AP. *In situ* Raman spectra were recorded simultaneously using a Raman microscope (Teledyne Princeton Instruments IsoPlane 81, USA). FEI Technai G2 sprit TWIN, USA model high-resolution transmission electron microscope (HR-TEM) equipped with energy dispersive X-ray spectroscopy (EDS) was utilized to characterize the surface morphological structure, particle size and distribution, and materials purity of the Au and Ag NPs.

2.4. Catalytic reduction of 4-NP

The catalytic reaction of 4-NP reduction over the synthesized Au NPs was performed in the container-free acoustic levitator system. For instance, 50 μL of 4-NP pollutant mixed with $NaBH_4$ (0.1 M 4-NP + 1 mM $NaBH_4$ solution in deionized water) was placed into acoustic levitation by a micropipette, and the droplet was levitated between the ultrasonic emitter and reflector. Then, the 10-μL colloidal solution of Au NPs dispersed in deionized water was added to the levitated pollutant

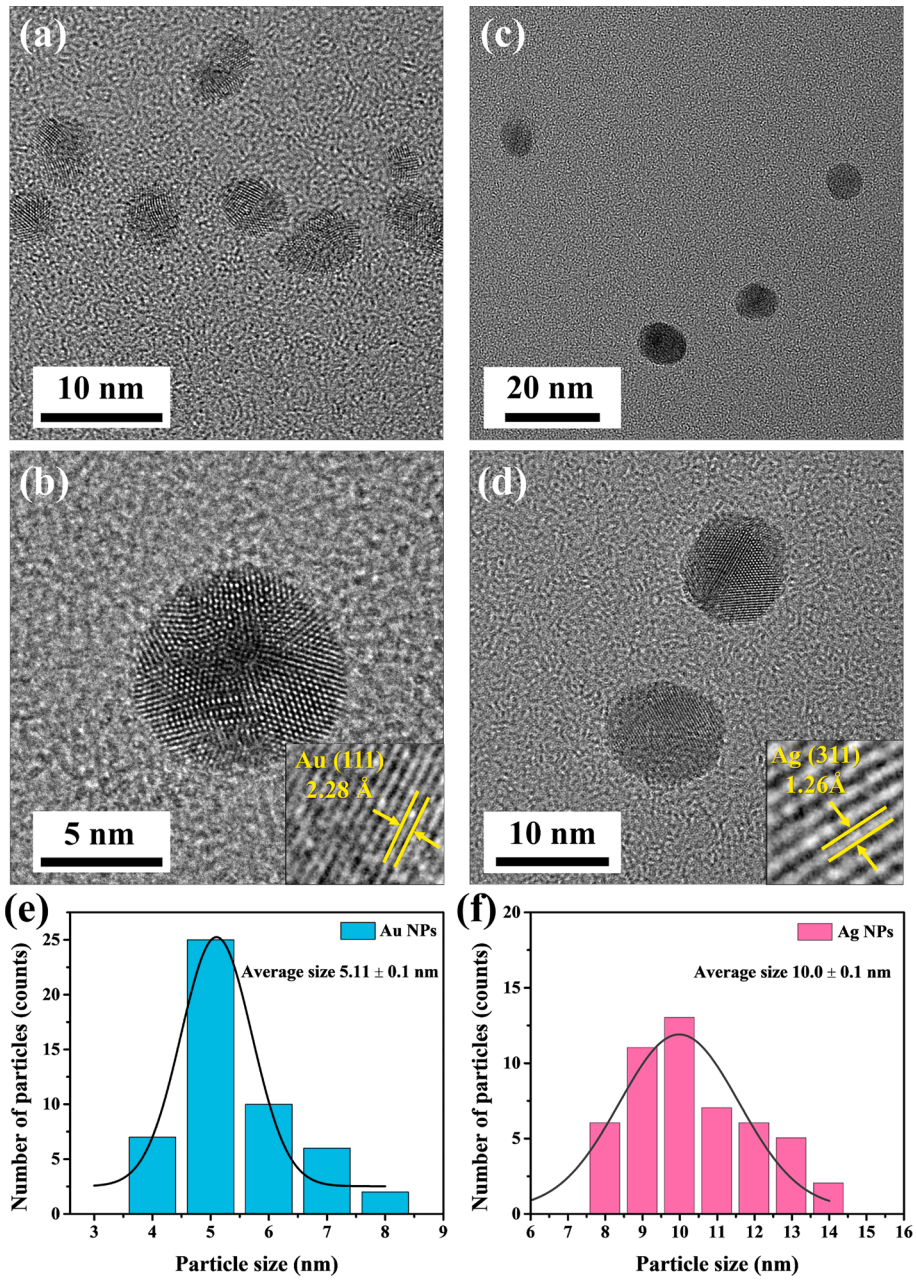

Fig. 4. HR-TEM images of (a and b) Au NPs and (c and d) Ag NPs (inset of Figure b and d shows the *d*-spacing of Au and Ag NPs). (e and f) Particle size distribution of Au and Ag NPs synthesized via acoustic levitation with PLI process.

Table 1
Comparison of particle size, reaction time for catalyst formation, and catalytic performance of Au NPs synthesized via acoustic levitation coupled with PLI with recently reported catalysts synthesized using other chemical synthetic routes.

S.No	Catalyst	Synthesis route	Reaction Time	Particle size	4-NP reduction (complete reduction time)	Reference
1	Au NPs	PLI in levitator	2 min	5.11 ± 0.1 nm	8 min	This study
2	Hollow Au NPs	Sol–gel process	10 min	56 ± 6 nm	34 min	[39]
3	GO/Au-Fe3O4 NPs	Coprecipitation method	24 h	57.53 nm	15 min	[40]
4	Au/AC	Homogeneous deposition–precipitation method	14 h	7.95 nm	30 min	[41]
5	Au NPs	Citrate thermal reduction technique	10 min	24.1 nm	14 min	[42]
6	Ag/GO NPs	Chemical method	15 min	7.5 nm	25 min	[43]

droplet. Ultrasonic levitation may help in uniformly mixing the catalyst and the pollutant. After adding the Au NPs, the catalytic reaction was initiated, and thus the initial time was considered the zero point in the catalytic 4-NP reduction kinetic experiments. The catalytic reaction continued for 8 min, and simultaneously the reduction and conversion of 4-NP to 4-AP was monitored via *in situ* UV–Vis and Raman spectroscopy coupled with an acoustic levitator system. For comparison, we also performed control experiment without the addition of NPs.

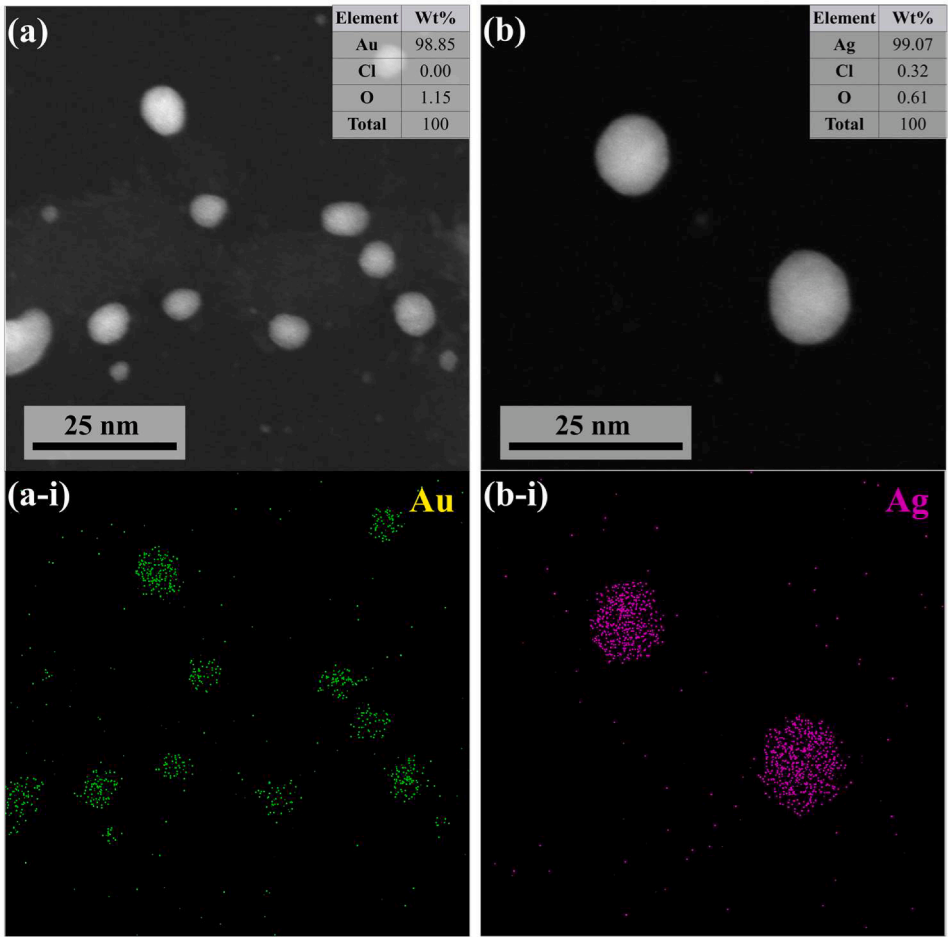

Fig. 5. EDS mapping and composition of (a and a-i) Au NPs and (b and b-i) Ag NPs synthesized via acoustic levitation with PLI process.

3. Results and discussion

3.1. Function of the acoustic levitator

Fig. 1 shows a typical schematic of the acoustic levitator system. As mentioned in the experimental section, a tec5 AG acoustic levitator (Germany) was used herein. The transducer generates ultrasonic sound waves with a frequency of 58 kHz and sound pressure level of 166 dB (4 W/cm^2) that are reflected by a resonance-tuned concave mirror. A standing wave with equally spaced nodes and antinodes is generated by multiple reflections between the transducer and the reflector. The levitated droplet can be suspended when a droplet is inserted around a pressure node of the acoustic standing wave [29,30]. The sample weight is balanced by the acoustic radiation pressure from below and kept concentrically by the circumferential Bernoulli force. Therefore, the levitated droplets are smaller than the diameter of sound and are located below the pressure minima of an ultrasonic standing wave. In our tec5 AG ultrasonic levitator system, the distance between the transducer and reflector can be adjusted with a micrometer (minimum ~ 10 mm to 29 mm). However, we fixed the distance between the transducer and reflector of ~ 16 mm for this study. The wavelength of a sound wave can be calculated using the relation $\lambda = c/f$, where λ, c, and f are the wavelength of sound wave (mm), speed of sound in air which is a constant value (~343 m/s), and frequency of the transducer (58 kHz), respectively [31]. The calculated wavelength is 5.9 mm, and wavelength is also measured as the distance between two nodes (half of the wavelength is one node ~ 2.95 mm). The distance between the transducer and reflector is ~ 16 mm; thus, the standing wave can generate approximately 5 nodes and 4 antinodes.

Both power supplies provide 10-W electric power with sound pressure levels up to ~ 166 dB (4 W/cm^2) for the 58-kHz levitator, which can be adjusted with the amplitude of the transducer's oscillations. Therefore, under ambient conditions, this is sufficient to levitate 3-mm diameter droplets at 58 kHz and can levitate liquid or solid samples of various sizes. Besides, it can float small single crystals and aggregated samples as well as liquids and solids. A sample with a minimum diameter of 2 μm can be floated, and a sample with a maximum diameter of 3 mm and a volume of approximately 70–100 μL can also be floated. The sample levitated through acoustic levitation is container-less and has no interaction with the container; thus it is suitable for various reaction experiments. The distinctive environment advanced by acoustic levitation, such as container-less chamber and droplet, may produce unique chemical and physical effects. Specifically, acoustic levitation can be utilized at low to high temperatures, like 218 to 2700 K, which enables a synthetic method for multiphase reactions [3,32].

3.2. Formation mechanism of Au and Ag NPs

The synthesis process of Au and Ag NPs in an acoustic levitator is mainly based on the PLI process coupled with acoustic levitation (**video SV1**). Fig. 2**a** illustrates the detailed schematic synthesis process**.** The free-standing wave field formed between the ultrasonic levitator emitter and reflector facilitates floating the sample to accomplish levitation (Fig. 2**b**) [5]. The formation of metal NPs occurs during the PLI process of the acoustic-levitated droplet of the corresponding metal salt solution without any external reducing reagent and, thus, attributed to the methanol solvent decomposition by optical acceleration. Upon the PLI, methanol decomposed to yield $CH_3^{\bullet}$ and $H^{\bullet}$ radicals, which act as

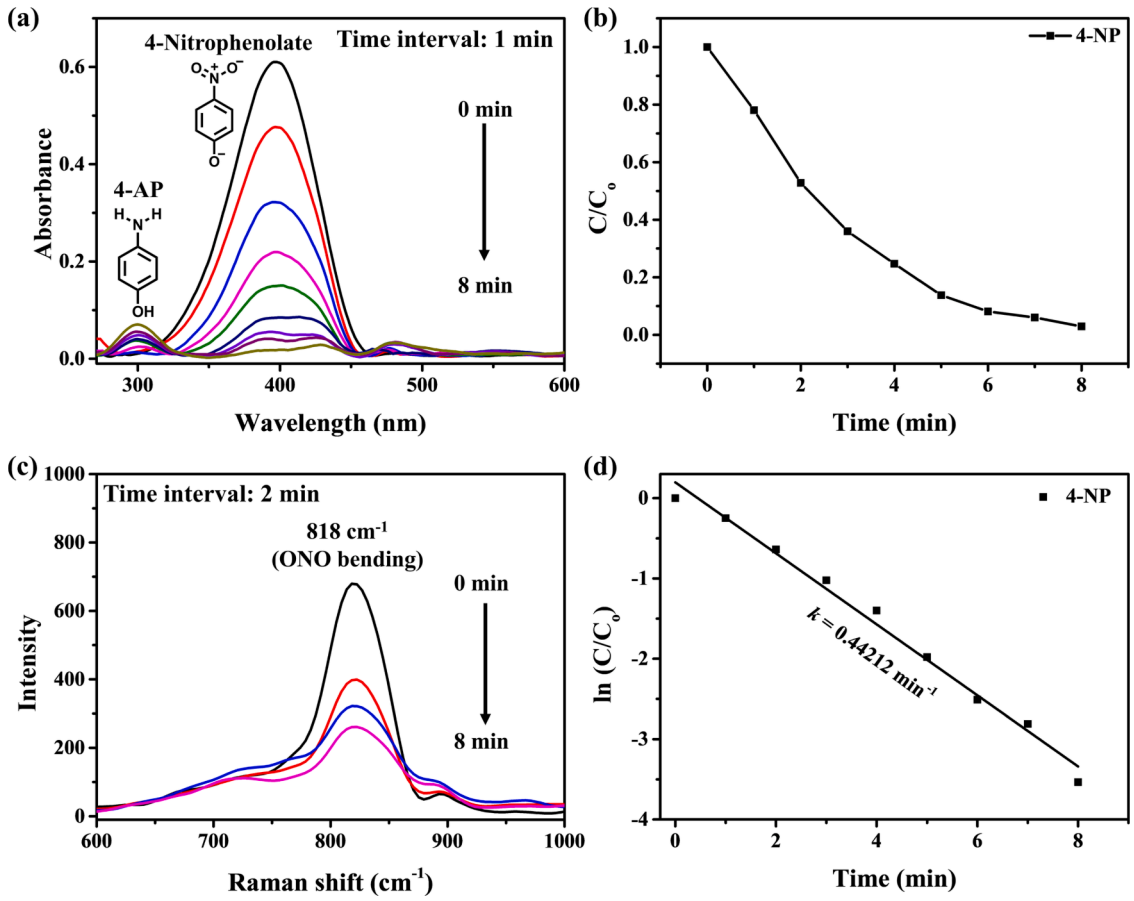

Fig. 6. Catalytic activity of Au NPs synthesized via acoustic levitation with PLI process toward 4-NP reduction into 4-AP: (a) time-dependent *in situ* UV–Vis spectra of 4-NP reduction, (b) complete reduction of 4-NP concentration in 8 min, (c) time-dependent *in situ* Raman spectra of 4-NP reduction, and (d) kinetics of pseudo-first order plot of ln (C/C_0) versus time for 4-NP reduction reaction over synthesized Au NPs.

reducing agents [17,19]. Fig. 2**c** shows the UV–Vis absorption spectra of 10 mM Au metal salt solution and Au NPs. A distinctive surface plasmon resonance (SPR) peak for the resulting Au NPs appeared at ~ 532 nm after the PLI of Au metal salt, suggesting rapid Au^{3+} reduction (~301 nm) to form Au NPs (~532 nm) [33]. In contrast, the SPR absorption peak of Ag NPs appeared at ~ 401 nm upon PLI of the Ag^+ salt solution (~247 nm) to form Ag NPs via reduction (Fig. 2**d**).

A high-resolution camera was used to capture the real image of the levitated droplet during reduction of metal salts into Au and Ag NPs (Fig. 3**a** and **b**). Consequently, the transparent color of the levitated metal salt droplet turned violet and yellow after PLI, facilitating the formation of Au and Ag NPs, respectively. Au^{3+} and Ag^+ reduction kinetics was investigated by monitoring the SPR intensity peak concerning the PLI time. The SPR peaks corresponding to Au and Ag NPs appeared immediately after PLI of corresponding metal salts, and the absorption peak intensity rapidly increased with the PLI duration time, with a significant blue shift (Fig. 3**c** and **d**). We observed that the metal salts were reduced within 40 s of the PLI process, and the reaction was completed after 2 min of the PLI duration. The blue shift in the wavelength of SPR peaks for the Au NPs (Fig. 3**c**) and Ag NPs (Fig. 3**d**) synthesized via acoustic levitation coupled with PLI indicated that the particle size was smaller [34]. As previously mentioned, the main drawback of several synthetic chemical reduction routes is the extended time required, which also necessitates constant stirring and heating. Moreover, citrate or $NaBH_4$ are commonly used as reducing agents for producing Au and Ag NPs [35]. Acoustic levitation coupled with PLI employed herein as a nontoxic and clean approach for producing Au and Ag NPs is a faster technique than other chemical reduction routes. Moreover, it proceeds without external reducing agents, stirring, and heating. This technique not only affords a sharp decrease in reaction time but also facilitates simultaneous monitoring of reactions via *in situ* spectroscopic studies, which indicates its high potential for numerous commercial applications [33].

Additionally, HR-TEM analysis was performed to examine the accurate particle size and distribution of Au, and Ag NPs synthesized using the acoustic levitation system coupled with PLI (Fig. 4). The surface morphological structure of the Au NPs (Fig. 4a and b) and Ag NPs (Fig. 4c and d) shows an identical spherical shape with uniform size distribution. Thus, the exhibited *d*-spacing value of 2.28 Å corresponds to the (1 1 1) plane of Au NPs (inset of Fig. 4**b**), whereas 1.26 Å results in the (3 1 1) plane of Ag NPs (inset of Fig. 4**d**). The HR-TEM results, therefore, validate the formation of Au and Ag NPs and support the UV–Vis absorption measurements. The particle size distribution is shown in Fig. 3e and 3f; the average particle size was estimated according to Gaussian fitting using HR-TEM images of Au and Ag NPs.

Furthermore, the average size of Au NPs synthesized using the acoustic levitation system coupled with the PLI process is ~ 5.11 nm (Fig. 4**e**), and the size of Ag NPs is ~ 10 nm (Fig. 4**f**). The free-standing wave field produced in acoustic levitation may afford uniform size distribution without particle aggregation and smaller particle size of the synthesized Au and Ag NPs compared with other chemical synthesis routes. The particle size and reaction time for forming the Au NPs synthesized in this study are superior to those reported for Au and Ag NPs synthesized using recently reported chemical synthesis routes (Table 1). Additionally, the EDS mapping and composition analysis revealed the formation of high-purity Au NPs (Fig. 5**a** and **b**) and Ag NPs (Fig. 5**c** and **d**) with uniform particle distribution with no other impurities.

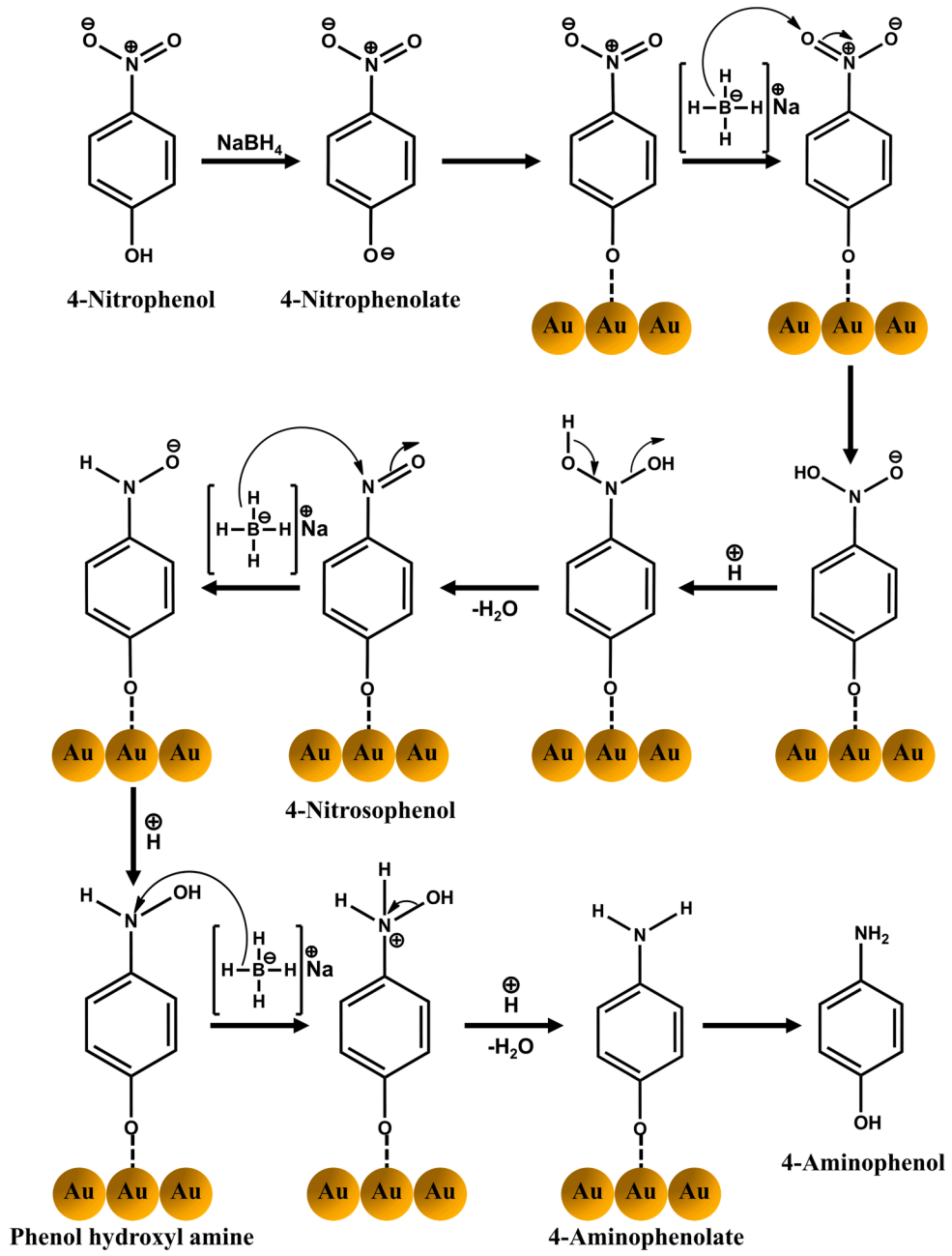

Fig. 7. Detailed catalytic reduction mechanism of 4-NP over Au NPs synthesized via acoustic levitation coupled with PLI.

3.3. *Catalytic reduction of 4-NP*

Using reduction of 4-NP to 4-AP as a standard catalytic reaction and $NaBH_4$ as a reducing agent, the catalytic characteristics of the Au NPs synthesized via acoustic levitation coupled with PLI were examined. The catalytic reaction was conducted in a container-less acoustic levitation chamber, and the reaction progress was monitored and confirmed by *in situ* spectroscopy (UV–Vis spectroscopy and Raman spectroscopy)-acoustic levitation at an optimized reaction condition. Approximately 50 μL of 4-NP with $NaBH_4$ was placed into acoustic levitation, and 10 μL of Au NP colloidal solution was added to the levitated droplet. Ultrasonic levitation aids the formation of a uniform reaction mixture. $NaBH_4$ is relatively ecofriendly due to the less toxicity of borates. $NaBH_4$ is basic in nature; hence, it abstracts the phenolic proton of 4-NP and forms 4-nitrophenolate anion, which is confirmed by the absorption peak of 4-nitrophenolate ion at ~ 397 nm (Fig. 6**a**). Without adding the Au NPs, no catalytic reaction occurred in the controls (**Figure S2**). When Au NPs were added, the resulting 4-nitrophenolate ion was initially adsorbed onto the Au NPs catalyst, where it was reduced to 4-AP in a series of steps for 8 min (Fig. 6**a** and **b**). The absorption peak intensity at ~ 397 nm decreased rapidly, indicating the reduction of 4-NP. Moreover, a new absorption peak at ~ 300 nm confirmed the resulting 4-AP product formation [36,37].

Additionally, the *in situ* Raman spectra collected confirmed the reduction of 4-NP over Au NPs (Fig. 6**c**). The Raman peaks for 4-NP at 818 cm^{-1} agree with a previous report [38]. Thus, the Raman peak intensities of 4-NP decreased with the catalytic reaction time from 0 to 8 min, revealing the reduction of 4-NP over Au NPs. Besides, the kinetic rate constant (k) for the catalytic reduction of 4-NP to 4-AP over Au NPs was calculated using a pseudo-first-order kinetic reaction model: $kt = \ln(C_t/C_0)$, where k is the apparent kinetic rate constant (min^{-1}), C_t is the pollutant concentration at various time (t) intervals, and C_0 is the

pollutant concentration at the initial point (Fig. 6**d**) [21]. Thus, the estimated k-value for the catalytic 4-NP reduction was ~ 0.0442 min^{-1}, suggesting that the catalytic activity of Au NPs obtained via acoustic levitation with the PLI process is comparable, if not superior to those reported by previous studies on catalysts synthesized using other chemical routes (Table 1).

Fig. 7 depicts the detailed catalytic reduction mechanism of 4-NP over Au NPs. The electrophilicity of the nitro group increases once it is adsorbed onto the Au surface because of the electropositive nature of Au, which helps in hydride ion abstraction from $NaBH_4$. Electron delocalization in the nitro group occurs after abstraction of the hydride ion, affording formation of anionic N,N-di hydroxyl amino phenolate, which then abstracts a proton from the solvent to form N,N-di hydroxyl amine intermediate, which later yields nitroso phenol when water is eliminated. Thus, the formed nitroso phenol is further reduced to phenol hydroxyl amine by the hydride ion (from $NaBH_4$) followed by proton abstractions. As generated phenol hydroxyl amine is converted to a 4-amino phenolate ion by protonation followed by water molecule elimination. Finally, the 4-amino phenolate ion is desorbed by the Au NPs surface and affords formation 4-aminophenol [44,45].

4. Conclusion

Herein, Au and Ag NPs were synthesized via acoustic levitation coupled with PLI without external reducing agents or surfactants. The growth and formation of NPs were simultaneously monitored via *in situ* UV–Vis and Raman spectroscopy. A photoreduction reaction mechanism is proposed to understand the reduction pathway of metal salts into corresponding metal NPs in acoustic-levitated space by the PLI process. Besides, the benefit of container-free sample handling by levitating process lies in the elimination of the complicating impacts caused by the contacting wall or surface on the sample, continuous cavitation effect, and bubble movement on the levitated droplet. Also, utilizing a fixed ultrasonic standing wave also accelerates the nucleation and controls the growth of the particle size. The catalytic activity when considering 4-NP reduction as a standard catalytic reaction reveals that the Au NPs synthesized in a container-free acoustic levitator via PLI exhibit excellent performance through the reduction of 4-NP into 4-AP with a rate constant of ~ 0.0442 min^{-1} in 8 min. We believe this concept adopted herein will open new avenues for exploring extensive nanomaterials and studying chemical reactions significant to material science, chemistry, biology, and medical fields.

CRediT authorship contribution statement

Juhyeon Park: Conceptualization, Investigation, Data curation. **Ahreum Min:** Conceptualization, Investigation. **Jayaraman Theerthagiri:** Conceptualization, Investigation, Writing – review & editing. **Muthupandian Ashokkumar:** Conceptualization, Investigation, Writing – review & editing. **Myong Yong Choi:** Supervision, Funding acquisition, Project administration, Writing – review & editing.

Declaration of Competing Interest

The authors declare that they have no known competing financial interests or personal relationships that could have appeared to influence the work reported in this paper.

Acknowledgements

This research was supported by Korea Basic Science Institute (National research Facilities and Equipment Center) grant funded by the Ministry of Education. (No. 2019R1A6C1010042, 2021R1A6C103A427). The authors acknowledge the financial support from National Research Foundation of Korea (NRF), (2022R1A2C2010686, 2022R1A4A3033528, 2019H1D3A1A01071209, 2021R1C1C2010726, 2021R1I1A1A01060380).

Appendix A. Supplementary data

Supplementary data to this article can be found online at https://doi.org/10.1016/j.ultsonch.2023.106345.

References

[1] Q. Shi, W. Di, D. Dong, L.W. Yap, L. Li, D. Zang, W. Cheng, A General Approach to Free-Standing Nanoassemblies via Acoustic Levitation Self-Assembly, ACS Nano 13 (2019) 5243–5250.
[2] J. Schenk, L. Tröbs, F. Emmerling, J. Kneipp, U. Panne, M. Albrecht, Simultaneous UV/Vis spectroscopy and surface enhanced Raman scattering of nanoparticle formation and aggregation in levitated droplets, Anal. Methods 4 (2012) 1252–1258.
[3] J. Leiterer, F. Delißen, F. Emmerling, A.F. Thünemann, U. Panne, Structure analysis using acoustically levitated droplets, Anal. Bioanal. Chem. 391 (2008) 1221–1228.
[4] B.B. Dangi, D.J. Dickerson, Design and Performance of an Acoustic Levitator System Coupled with a Tunable Monochromatic Light Source and a Raman Spectrometer for In Situ Reaction Monitoring, ACS Omega 6 (2021) 10447–10453.
[5] Y. Zheng, Q. Zhuang, Y. Ruan, G. Zhu, W. Xie, Y. Jiang, H. Li, B. Wei, Floating synthesis with enhanced catalytic performance via acoustic levitation processing, Ultrason. Sonochem. 87 (2022), 106051.
[6] M.A.B. Andrade, N. Pérez, J.C. Adamowski, Review of Progress in Acoustic Levitation, Braz. J. Phys. 48 (2018) 190–213.
[7] S.J. Brotton, R.I. Kaiser, Controlled Chemistry via Contactless Manipulation and Merging of Droplets in an Acoustic Levitator, Anal. Chem. 92 (2020) 8371–8377.
[8] B. Baruah, G.J. Gabriel, M.J. Akbashev, M.E. Booher, Facile Synthesis of Silver Nanoparticles Stabilized by Cationic Polynorbornenes and Their Catalytic Activity in 4-Nitrophenol Reduction, Langmuir 29 (2013) 4225–4234.
[9] G. Bharath, J. Prakash, K. Rambabu, G.D. Venkatasubbu, A. Kumar, S. Lee, J. Theerthagiri, M.Y. Choi, F. Banat, Synthesis of TiO_2/RGO with plasmonic Ag nanoparticles for highly efficient photoelectrocatalytic reduction of CO_2 to methanol toward the removal of an organic pollutant from the atmosphere, Environ. Pollut. 281 (2021), 116990.
[10] S.H. Lee, H.J. Jung, S.J. Lee, J. Theerthagiri, T.H. Kim, M.Y. Choi, Selective synthesis of Au and graphitic carbon-encapsulated Au (Au@GC) nanoparticles by pulsed laser ablation in solvents: Catalytic Au and acid-resistant Au@GC nanoparticles, Appl. Surf. Sci. 506 (2020), 145006.
[11] Á.d.J. Ruíz-Baltazar,, Sonochemical activation-assisted biosynthesis of Au/Fe_3O_4 nanoparticles and sonocatalytic degradation of methyl orange, Ultrason. Sonochem. 73 (2021), 105521.
[12] Z. Mohammadi, M.H. Entezari, Sono-synthesis approach in uniform loading of ultrafine Ag nanoparticles on reduced graphene oxide nanosheets: An efficient catalyst for the reduction of 4-Nitrophenol, Ultrason. Sonochem. 44 (2018) 1–13.
[13] Y. Yu, S.S. Naik, Y. Oh, J. Theerthagiri, S.J. Lee, M.Y. Choi, Lignin-mediated green synthesis of functionalized gold nanoparticles via pulsed laser technique for selective colorimetric detection of lead ions in aqueous media, J. Hazard. Mater. 420 (2021), 126585.
[14] L. Gao, S. Mei, H. Ma, X. Chen, Ultrasound-assisted green synthesis of gold nanoparticles using citrus peel extract and their enhanced anti-inflammatory activity, Ultrason. Sonochem. 83 (2022), 105940.
[15] C. Gutiérrez-Wing, R. Esparza, C. Vargas-Hernández, M.E. Fernández García, M. José-Yacamán, Microwave-assisted synthesis of gold nanoparticles self-assembled into self-supported superstructures, Nanoscale 4 (2012) 2281–2287.
[16] J. Theerthagiri, R.A. Senthil, D. Thirumalai, J. Madhavan, Sonophotocatalytic Degradation of Organic Pollutants Using Nanomaterials, Handbook of Ultrasonics and Sonochemistry, Springer Singapore, Singapore, 2016, pp. 553-586.
[17] Y. Yu, S.J. Lee, J. Theerthagiri, Y. Lee, M.Y. Choi, Architecting the AuPt alloys for hydrazine oxidation as an anolyte in fuel cell: Comparative analysis of hydrazine splitting and water splitting for energy-saving H_2 generation, Environmental, Applied Catalysis B, 2022, p. 121603.
[18] S.S. Naik, S.J. Lee, J. Theerthagiri, Y. Yu, M.Y. Choi, Rapid and highly selective electrochemical sensor based on ZnS/Au-decorated f-multi-walled carbon nanotube nanocomposites produced via pulsed laser technique for detection of toxic nitro compounds, J. Hazard. Mater. 418 (2021), 126269.
[19] Y. Yu, J. Theerthagiri, S.J. Lee, G. Muthusamy, M. Ashokkumar, M.Y. Choi, Integrated technique of pulsed laser irradiation and sonochemical processes for the production of highly surface-active NiPd spheres, Chem. Eng. J. 411 (2021), 128486.
[20] Y. Yu, A. Min, H.J. Jung, J. Theerthagiri, S.J. Lee, K.-Y. Kwon, M.Y. Choi, Method development and mechanistic study on direct pulsed laser irradiation process for highly effective dechlorination of persistent organic pollutants, Environ. Pollut. 291 (2021), 118158.
[21] T. Begildayeva, S.J. Lee, Y. Yu, J. Park, T.H. Kim, J. Theerthagiri, A. Ahn, H. J. Jung, M.Y. Choi, Production of copper nanoparticles exhibiting various morphologies via pulsed laser ablation in different solvents and their catalytic activity for reduction of toxic nitroaromatic compounds, J. Hazard. Mater. 409 (2021), 124412.
[22] J. Theerthagiri, K. Karuppasamy, S.J. Lee, R. Shwetharani, H.-S. Kim, S.K.K. Pasha, M. Ashokkumar, M.Y. Choi, Fundamentals and comprehensive insights on pulsed

laser synthesis of advanced materials for diverse photo- and electrocatalytic applications 11 (2022) 250.
[23] T. Begildayeva, J. Theerthagiri, S.J. Lee, Y. Yu, M.Y. Choi, Unraveling the Synergy of Anion Modulation on Co Electrocatalysts by Pulsed Laser for Water Splitting: Intermediate Capturing by In Situ/Operando Raman Studies, Small, n/a (2022) 2204309.
[24] S. Yeon, S.J. Lee, J. Kim, T. Begildayeva, A. Min, J. Theerthagiri, M.L.A. Kumari, L. M.C. Pinto, H. Kong, M.Y. Choi, Sustainable removal of nitrite waste to value-added ammonia on Cu@Cu_2O core–shell nanostructures by pulsed laser technique, Environ. Res. 215 (2022), 114154.
[25] S. Denrah, M. Sarkar, Design of experiment for optimization of nitrophenol reduction by green synthesized silver nanocatalyst, Chem. Eng. Res. Des. 144 (2019) 494–504.
[26] J. Theerthagiri, J. Madhavan, S.J. Lee, M.Y. Choi, M. Ashokkumar, B.G. Pollet, Sonoelectrochemistry for energy and environmental applications, Ultrason. Sonochem. 63 (2020), 104960.
[27] J. Madhavan, J. Theerthagiri, D. Balaji, S. Sunitha, M.Y. Choi, M. Ashokkumar, Hybrid Advanced Oxidation Processes Involving Ultrasound: An Overview, Molecules (2019).
[28] J. Theerthagiri, S.J. Lee, K. Karuppasamy, S. Arulmani, S. Veeralakshmi, M. Ashokkumar, M.Y. Choi, Application of advanced materials in sonophotocatalytic processes for the remediation of environmental pollutants, J. Hazard. Mater. 412 (2021), 125245.
[29] Z. Fang, X. Huang, M.E. Taslim, K.-T. Wan, Flexural bending resonance of acoustically levitated glycerol droplet, Phys. Fluids 33 (2021), 071701.
[30] K. Hasegawa, Y. Abe, A. Goda, Microlayered flow structure around an acoustically levitated droplet under a phase-change process, npj Microgravity 2 (2016) 16004.
[31] T. Matsubara, K. Takemura, Containerless Bioorganic Reactions in a Floating Droplet by Levitation Technique Using an Ultrasonic Wave, Adv. Sci. 8 (2021) 2002780.
[32] D. Zang, Y. Yu, Z. Chen, X. Li, H. Wu, X. Geng, Acoustic levitation of liquid drops: Dynamics, manipulation and phase transitions, Adv. Colloid Interface Sci. 243 (2017) 77–85.
[33] A. Gangula, R. Podila, R. M, L. Karanam, C. Janardhana, A.M. Rao,, Catalytic Reduction of 4-Nitrophenol using Biogenic Gold and Silver Nanoparticles Derived from Breynia rhamnoides, Langmuir 27 (2011) 15268–15274.
[34] S.L. Kleinman, B. Sharma, M.G. Blaber, A.-I. Henry, N. Valley, R.G. Freeman, M. J. Natan, G.C. Schatz, R.P. Van Duyne, Structure Enhancement Factor Relationships in Single Gold Nanoantennas by Surface-Enhanced Raman Excitation Spectroscopy, J. Am. Chem. Soc. 135 (2013) 301–308.
[35] J. Theerthagiri, S.J. Lee, K. Karuppasamy, J. Park, Y. Yu, M.L.A. Kumari, S. Chandrasekaran, H.-S. Kim, M.Y. Choi, Fabrication strategies and surface tuning of hierarchical gold nanostructures for electrochemical detection and removal of toxic pollutants, J. Hazard. Mater. 420 (2021), 126648.
[36] S. Khan, W. Runguo, K. Tahir, Z. Jichuan, L. Zhang, Catalytic reduction of 4-nitrophenol and photo inhibition of Pseudomonas aeruginosa using gold nanoparticles as photocatalyst, J. Photochem. Photobiol. B Biol. 170 (2017) 181–187.
[37] S. Noël, H. Bricout, A. Addad, C. Sonnendecker, W. Zimmermann, E. Monflier, B. Léger, Catalytic reduction of 4-nitrophenol with gold nanoparticles stabilized by large-ring cyclodextrins, New J. Chem. 44 (2020) 21007–21011.
[38] S. Mourdikoudis, V. Montes-García, S. Rodal-Cedeira, N. Winckelmans, I. Pérez-Juste, H. Wu, S. Bals, J. Pérez-Juste, I. Pastoriza-Santos, Highly porous palladium nanodendrites: wet-chemical synthesis, electron tomography and catalytic activity, Dalton Trans. 48 (2019) 3758–3767.
[39] I. Kalyan, T. Pal, A. Pal, Immobilization of size variable Au nanoparticles on surfactant-modified silica and their catalytic application toward 4-nitrophenol reduction: A comparative account of catalysis, Surf. Interfaces 26 (2021), 101423.
[40] J. Rawat, K. Bijalwan, C. Negi, H. Sharma, C. Dwivedi, Magnetically recoverable Au doped iron oxide nanoparticles coated with graphene oxide for catalytic reduction of 4-nitrophenol, Mater. Today:. Proc. 45 (2021) 4869–4873.
[41] A. Kumar, M. Belwal, R.R. Maurya, V. Mohan, V. Vishwanathan, Heterogeneous catalytic reduction of anthropogenic pollutant, 4-nitrophenol by Au/AC nanocatalysts, Materials Science for Energy Technologies 2 (2019) 526–531.
[42] N. Berahim, W.J. Basirun, B.F. Leo, M.R. Johan, Synthesis of Bimetallic Gold-Silver (Au-Ag) Nanoparticles for the Catalytic Reduction of 4-Nitrophenol to 4-Aminophenol, Catalysts 8 (2018) 412.
[43] T. Wu, L. Zhang, J. Gao, Y. Liu, C. Gao, J. Yan, Fabrication of graphene oxide decorated with Au–Ag alloy nanoparticles and its superior catalytic performance for the reduction of 4-nitrophenol, J. Mater. Chem. A 1 (2013) 7384–7390.
[44] Y.S. Seo, E.-Y. Ahn, J. Park, T.Y. Kim, J.E. Hong, K. Kim, Y. Park, Y. Park, Catalytic reduction of 4-nitrophenol with gold nanoparticles synthesized by caffeic acid, Nanoscale Res. Lett. 12 (2017) 7.
[45] K. Naseem, R. Begum, W. Wu, A. Irfan, J. Nisar, M. Azam, Z.H. Farooqi, Core/shell composite microparticles for catalytic reduction of p-nitrophenol: kinetic and thermodynamic study, Int. J. Environ. Sci. Technol. 18 (2021) 1809–1820.